DISTRIBUTION OF TRAPPED RADIATION IN THE GEOMAGNETIC FIELD

SEKIKO YOSHIDA

GEORGE H. LUDWIG

AND

JAMES A. VAN ALLEN

Distribution of Trapped
Radiation in the Geomagnetic Field[1]

SEKIKO YOSHIDA,[2] GEORGE H. LUDWIG,[3] AND JAMES A. VAN ALLEN

Department of Physics and Astronomy
State University of Iowa
Iowa City, Iowa

Abstract. The altitude dependence (360 to 2090 km) of the intensity of geomagnetically trapped radiation as measured with Explorer I (satellite 1958α) is given for a number of geographic locations. It is found that all intensity data in the vicinity of the magnetic dip equator and over the full range of longitude and of altitude can be represented satisfactorily by a single function of the scalar magnetic field intensity *B*. The value of *B* at the lower boundary of the inner zone of trapped radiation is a monotonically increasing function of magnetic dip latitude; such data from all available geographic locations are well represented by a single curve.

Introduction. Observations with satellites [*Van Allen, Ludwig, Ray, and McIlwain,* 1958; *Van Allen, McIlwain, and Ludwig,* 1959a; *Krassovsky, Kushnir, Vordovsky, Zokharov, and Svetlitsky,* 1958] and with space probes [*Van Allen and Frank,* 1959a; *Vernov, Chudakov, Vakulov and Logachev,* 1959; *Van Allen and Frank,* 1959b] have revealed the existence of large fluxes of high-energy and low-energy protons and electrons trapped in the geomagnetic field.

The present paper contains several new results of further analysis of the observations by Explorer I (satellite 1958α) during the period February 1 to March 15, 1958. Only those observations during magnetically quiet days ($K_p \leq 3$) have been used, since there are substantial temporal fluctuations in the distribution of intensity in the high-latitude edges of the inner zone and in the 'slot' between inner and outer zones (as well as in the outer zone, which was not encompassed by the Explorer I orbit). No other selection criteria were used except those necessary to assure reliable data.

Details of the apparatus of Explorer I have been published by *Ludwig* [1959]. The radiation detector was an Anton type 314 Geiger tube having an omnidirectional geometric factor $G_o = 17.4$ cm², a total shielding of 1.5 g/cm² of stainless steel, and an efficiency of 0.83 for fast charged particles which penetrate the effective volume directly. The shielding corresponded to the range of 30-Mev protons or to the extrapolated range of 3-Mev electrons. We have been able to extend considerably the dynamic range of the measurements reported previously by post-flight, experimental study of the characteristics of the counting system in the similar spare payload. It was found that the relation between apparent counting rate *r* and 'true' counting rate *R* (defined to be the rate of a system identical to the one used except having zero dead time) was well represented by the one-parameter formula $r = R \exp(-R\tau)$, whence $r(\max) = (e\tau)^{-1}$ at $R = (\tau)^{-1}$. For the spare payload $\tau = 244$ microseconds. The maximum observed rate in flight of Explorer I was 2200 counts per second. The relation between apparent and true counting rate was therefore taken to be of the above form with $\tau = 168$ microseconds, thus giving an $r(\max)$ equal to the flight value. By continuity of the data and by study of the statistical fluctuations of the apparent counting rate there was usually no difficulty in deciding which branch of the *r* versus *R* curve to read.

[2] On leave of absence from the Department of Physics, Nagoya University.

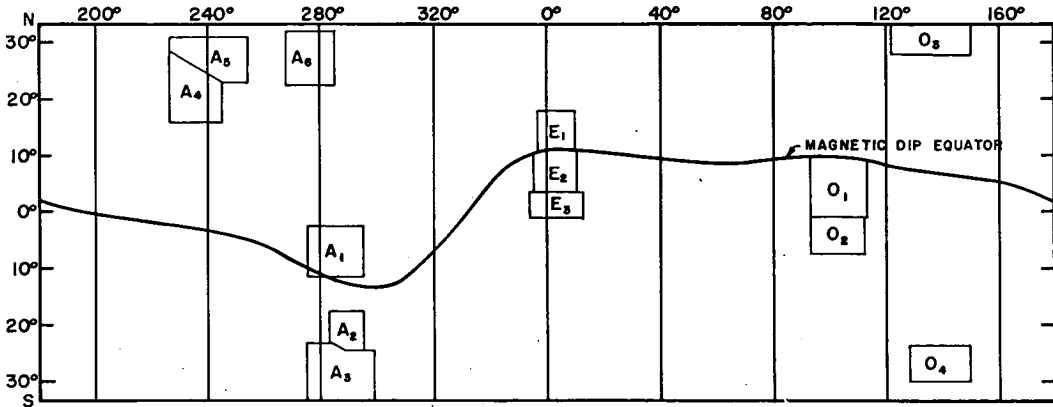[3] Research Fellow of U. S. Steel Foundation.

Fig. 1. Geographic regions of the earth over which observed data were used in the present paper. The magnetic dip equator and the magnetic dip angles used in obtaining entries of Table 1 are those of Chart 1700 of the U. S. Navy Hydrographic Office for the year 1955.

Organization of data. The basic tabulation of data listed the mean true counting rate of the Geiger tube over selected intervals of time (of typically about 12 seconds' duration) and the longitude, latitude, and altitude of the satellite at the center of the interval (to a positional accuracy of about ±10 km). The geographic regions of observation used in the present study are shown in Figure 1. Further details are listed in Table 1. All intensity data within each of the

13 regions O_1, O_2, O_3, O_4, E_1, E_2, E_3, A_1, A_2, A_3, A_4, A_5, and A_6 and within each altitude increment of 50 km were averaged and assigned to a weighted mean position within the corresponding volume element.

Analysis and interpretation. Figure 2 shows the altitude dependence of true counting rate in regions O_1, O_2, E_1, E_2, E_3, A_1, A_2, and A_3, for all of which the absolute value of the magnetic dip latitude is less than or equal to 19.0°. The mag-

TABLE 1.   Regions of Observation and Observed Lower Boundary of Inner Zone

| Region | Receiving Station | Position over the Earth | | | Lower Boundary of Inner Zone, at 100 counts/sec | |
		Geographic Longitude	Geographic Latitude	Magnetic Dip Latitude	Altitude, km	Scalar Magnetic Field Intensity B, gauss
O_1	Singapore	93.5°–113.9°E	9.5°N–1.0°S	0°–10.0°S	1360	0.216
O_2	Singapore	93.4°–112.4°E	1.0°–7.5°S	10.0°–19.0°S	1380	0.223
O_3	Tokyo	122.5°–150.0°E	28.0°–33.4°N	22.5°–27.5°N	1330	0.242
O_4	Woomera	128.5°–149.8°E	23.5°–30.0°S	35.0°–40.0°S	1480	0.290
E_1	Ibadan	3.0°W–10.5°E	18.0°–11.0°N	0°–8.0°N	890	0.216
E_2	Ibadan	5.0°W–10.5°E	11.0°–3.5°N	0°–10.0°S	830	0.214
E_3	Ibadan	5.7°W–12.7°E	3.5°N–1.0°S	10.0°–14.0°S	750	0.215
A_1	Quito, Antofa-gasta, Lima	84.3°–64.5°W	2.5°–11.5°S	0°–10.0°N	780	0.212
A_2	Antofagasta	76.4°–65.0°W	17.5°–24.5°S	2.5°–10.0°S	520	0.216
A_3	Santiago	84.6°–60.9°W	23.0°–33.4°S	10.0°–17.5°S	460	0.230
A_4	Pasadena	134.7°–114.9°W	16.0°–28.5°N	25.0–30.0°N	1200	0.253
A_5	Pasadena, Earth-quake Valley	133.6°–105.9°W	23.0°–31.0°N	30.0°–36.5°N	1150	0.273
A_6	Patrick A.F.B., Havana, Fort Stewart	92.5°–74.8°W	22.5°–32.0°N	35.0°–40.0°N	1130	0.292
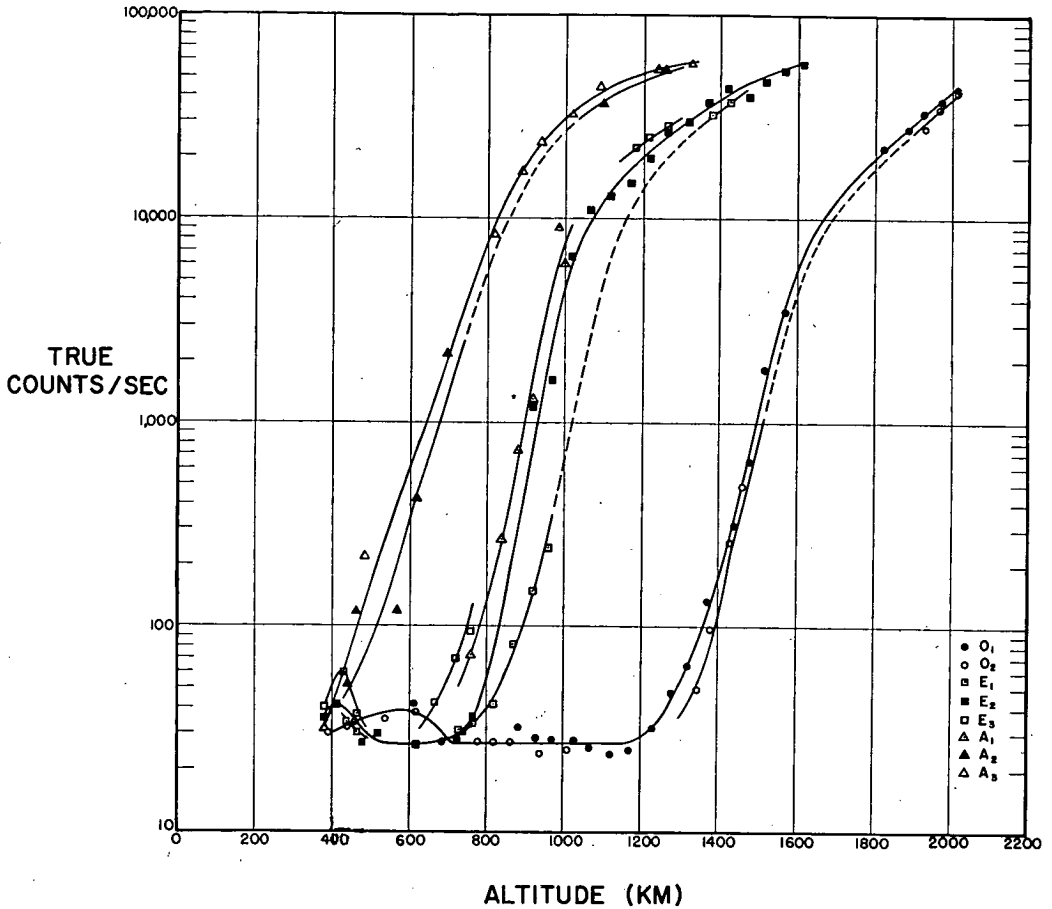
Fig. 2. True counting rate as a function of altitude over 8 geographic regions near the magnetic dip equator. The statistical standard error of each plotted point is less than 4 per cent, but there are larger systematic uncertainties at rates greater than 1000 counts per second inherent in the assumed relationship between apparent and true counting rates. Altitudes are accurate to ±10 km.

netic dip latitude λ_{dip}, defined by the dipole relationship $2 \tan \lambda_{dip} = \tan \delta$, where δ is the magnetic dip angle, has been shown empirically (P. Rothwell, private communication, 1959) to be a valuable parameter in systematizing the latitude dependence of intensity. However, the Rosenbluth [*Rosenbluth and Longmire*, 1957] integral invariant I has a clear theoretical basis [*Van Allen, McIlwain, and Ludwig*, 1959b] and will doubtless be a preferable parameter for this purpose when adequate tables become available.

Figure 2 clearly shows the way in which the altitude dependence of intensity changes with longitude for regions near the magnetic dip equator. The marked longitude effect was noted

in our earliest satellite work and was attributed to the displacement of the magnetic center of the earth from its geometric center. This interpretation has now been refined as detailed below.

The scalar intensity B of the real geomagnetic field was computed at 100-km-altitude intervals over each of the 13 regions of observation using the numerical values of *Finch and Leaton* [1957] for the 48 coefficients in the sixth-degree, sixth-order spherical harmonic representation of the magnetic potential [*Vestine, Lange, Laporte, and Scott*, 1947]. The first application of these values of B was the replotting of all counting-rate data of Figure 2 as a function of
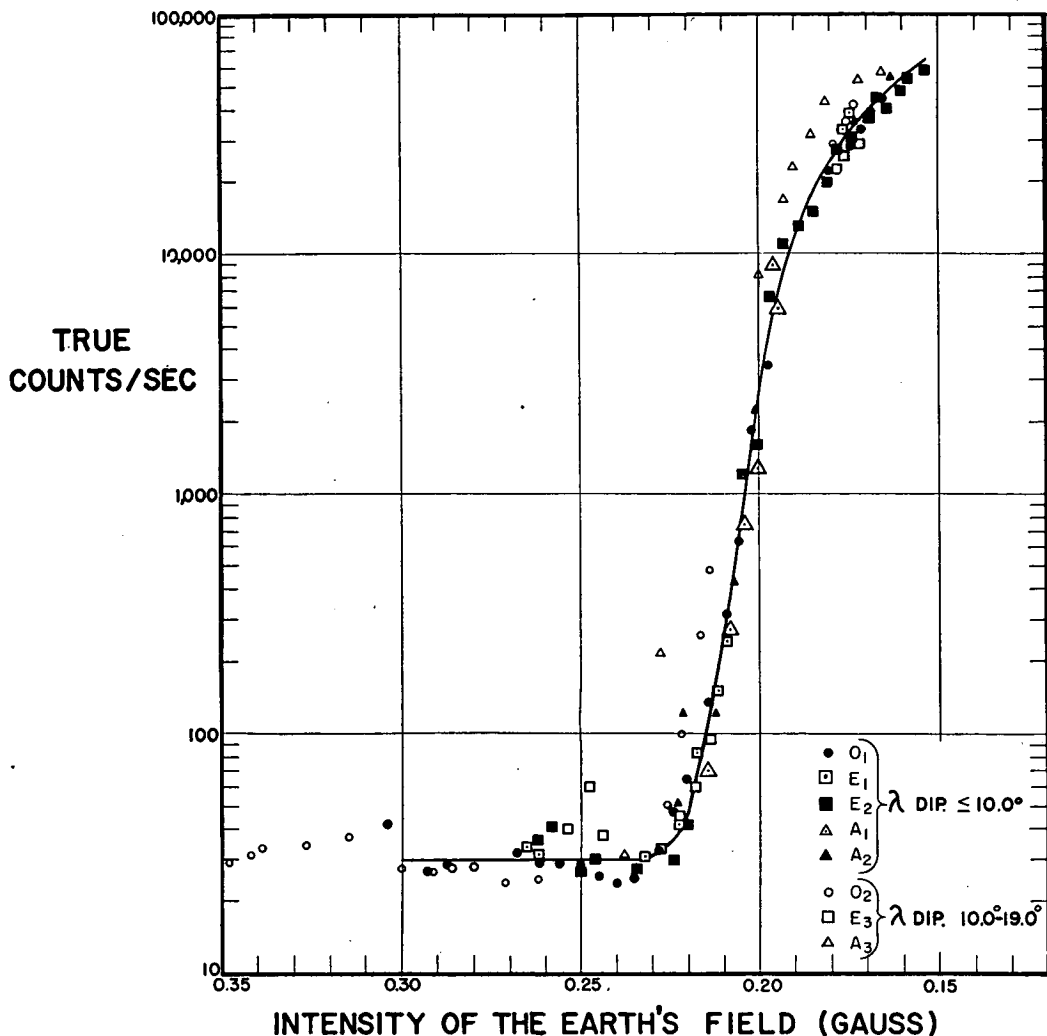
Fig. 3. Composite plot of all counting-rate data for which $|\lambda_{dip}| \leq 19.0°$ as a function of the computed scalar intensity B of the earth's field.

B (Fig. 3). It is seen from Figure 3 that all the radiation-intensity data in regions for which $|\lambda_{dip}| \leq 10°$ can be very well characterized by a single parameter, namely B. Thus, although loss mechanisms within the atmosphere provide the physical cause of the strong altitude dependence of intensity, Figure 3 shows that the longitude dependence of the intensity-altitude curves is completely accounted for by detailed features of the real geomagnetic field.

The effective displacement of the magnetic center of the earth from its geometric center is, from Figure 2 and Table 1, several hundred

kilometers. Since the atmosphere is concentric with the solid earth, the mirror points of trapped particles in a given magnetic shell within the inner zone occur deepest in the atmosphere at an approximate longitude of 310°E (and in the southern hemisphere). The dominant atmospheric contribution to scattering and energy loss presumably occurs near this longitude, as does the maximum 'outflux' of trapped particles. Observationally, such an effect would be evidenced by a more gradual tailing-out of the intensity toward higher values of B (i.e., toward lower altitudes) at the longi-

tude in question. No such longitudinal dependence can be discerned in Figure 3. It is concluded that the probability that a trapped particle is lost in one longitudinal precession around the earth is small. The particles that actuate the detector in the present experiment are protons of energies greater than 30 Mev and electrons of energies greater than 40 kev, the latter with low efficiency by way of their more penetrating bremsstrahlung. The trapped lifetimes of these particles in the central part of the inner zone are, therefore, long compared with their longitudinal precessional periods, which are of the order of minutes to hours. This result is to be expected in the light of previously published considerations which require much longer lifetimes. A special study of the outflux question is of considerable interest in its own right since it may provide an experimental determination of trapped lifetimes. Our data from Explorer IV (1958ϵ) and Explorer VII (1959ι) are being used for this study.

In the present paper it has been convenient to adopt as the lower boundary of the zone of trapped radiation that altitude at which the counting rate is 100 counts per second. In the vicinity of the magnetic dip equator the lower boundary of the inner radiation zone, as so defined, occurs (for the particular detector and absorber used in Explorer I) at a scalar field intensity of 0.215 gauss. (Perhaps a more generally satisfactory definition of the lower boundary is obtained by extrapolating the steeply rising part of the curve in Figure 3 to the cosmic-ray counting level, of 30 counts per second in this case. This process gives the lower boundary at $B = 0.220$ gauss.)

A study of counting-rate data at other magnetic dip latitudes was also made in the same manner as above. Figure 4 shows a replot of the smooth curve of Figure 3 and four other curves for the 5 cases, A_4, A_5, A_6, O_3, and O_4, for which the average λ_{dip} is $+28.0°$, $+34.5°$, $+38.5°$, $+25.5°$, and $-39.0°$, respectively. A single curve represents the two cases A_6 and O_4. Figure 4 reveals that the intensity structure of the
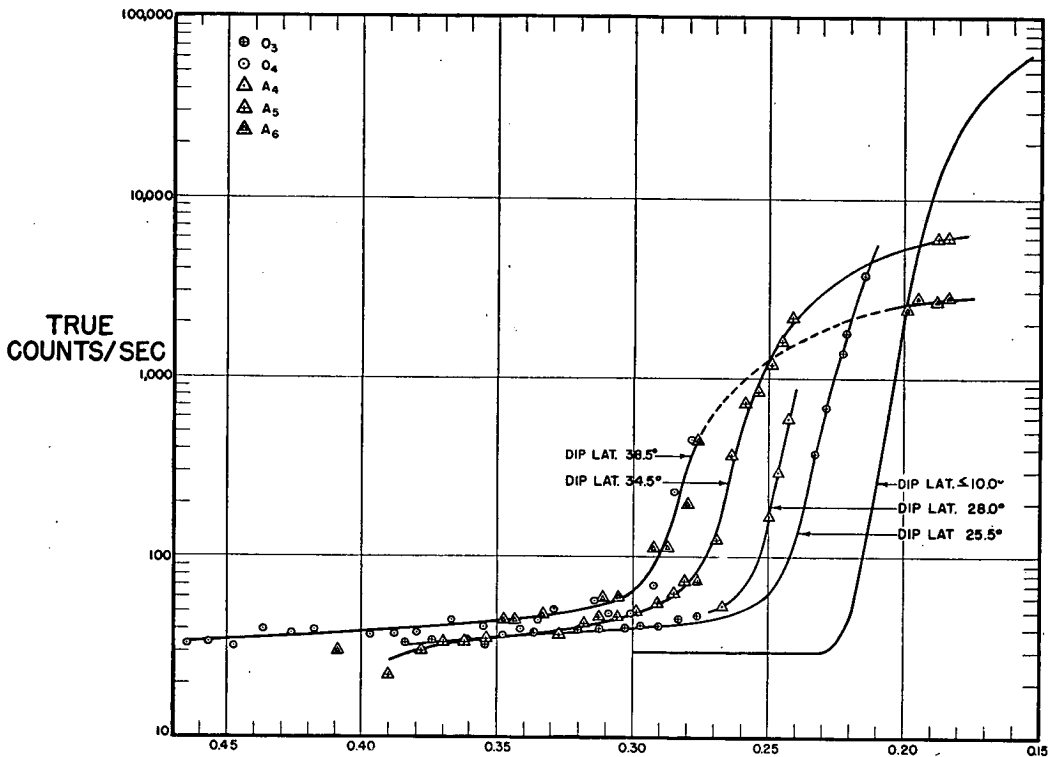

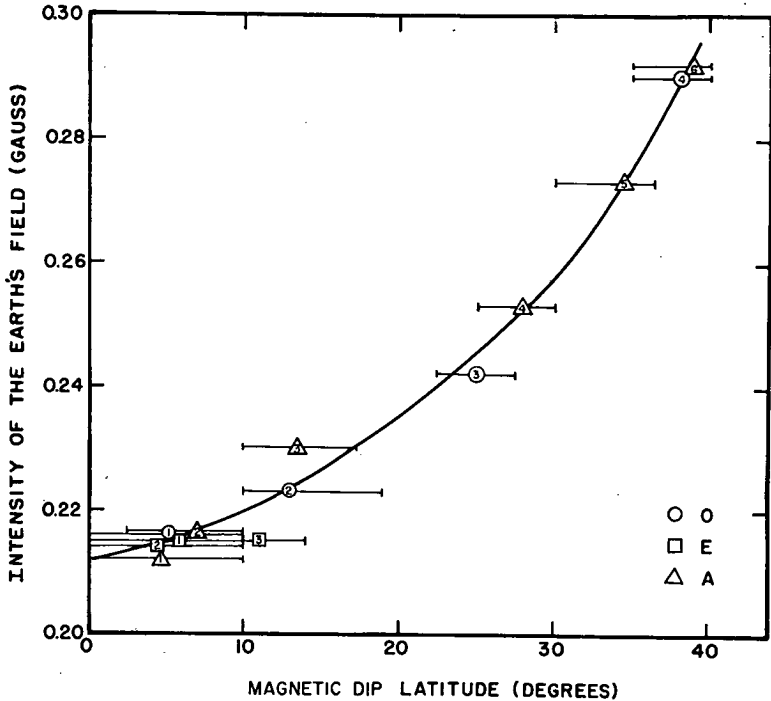Fig. 4. Counting rate versus B for 5 magnetic dip latitudes.

Fig. 5. Value of B at lower boundary of inner zone as a function of magnetic dip latitude.

trapped radiation changes in several respects as the latitude increases: (a) the lower boundary of the trapped-radiation region is less sharply defined than at the magnetic dip equator; (b) the lower boundary shifts to higher values of B; (c) the dependence of intensity on B is less rapid, and the maximum value of intensity decreases.

Point (b) is examined in more detail in Figure 5, which shows the value of B at which the lower boundary (100 counts per second) occurs as a function of magnetic dip latitude. See also Table 1. It is noteworthy that the data from all longitudes fit the same curve in Figure 5.

Figures 2, 3, 4, and 5 provide a convenient basis for estimating the radiation intensity at any desired point in the lower part of the inner zone. Such estimates are applicable only to a detector similar to the one used in this investigation.

REFERENCES

Finch, H. F., and B. R. Leaton, The earth's main magnetic field—epoch 1955.0, *Monthly Notices Roy. Astron. Soc. (Geophys. Suppl.)*, 7, 314–317, 1957.

Krassovsky, V. I., Y. M. Kushnir, G. A. Vordovsky, G. F. Zokharov, and E. M. Svetlitsky, Discovery of corpuscles with the help of the third artificial (Soviet) satellite of the earth, pp. 59–60 of Artificial Satellites of the Earth, no. 2, 82 pp., *Publ. Akad. Nauk SSSR*, Moscow, 1958.

Ludwig, G. H., Cosmic ray instrumentation in the first U. S. earth satellite, *Rev. Sci. Instr.*, 30, 223–229, 1959.

Rosenbluth, M. N., and C. L. Longmire, Stability of plasmas confined by magnetic fields, *Ann. Phys.*, 1, 120–140, 1957.

Van Allen, J. A., and L. A. Frank, Radiation around the earth to a radial distance of 107,400 km., *Nature*, 183, 430–434, 1959a.

Van Allen, J. A., and L. A. Frank, Radiation measurements to 658,300 km. with Pioneer IV, *Nature*, 184, 219–224, 1959b.

Van Allen, J. A., G. H. Ludwig, E. C. Ray, and C. E. McIlwain, Observation of high intensity radiation by satellites 1958α and γ, *Jet Propulsion*, 28, 588–592, 1958.

Van Allen, J. A., C. E. McIlwain, and G. H. Lud-

wig, Radiation observations with satellite 1958ε, *J. Geophys. Research, 64,* 271–286, 1959a.

Van Allen, J. A., C. E. McIlwain, and G. H. Ludwig, Satellite observations of electrons artificially injected into the geomagnetic field, *J. Geophys. Research, 64,* 877–891, 1959b.

Vernov, S. N., A. E. Chudakov, P. V. Vakulov, and Yu. I. Logachev, Study of terrestrial corpuscular radiation and cosmic rays during flight of the cosmic rocket, *Doklady Akad. Nauk SSSR, 125,* 304–307, 1959.

Vestine, E. H., I. Lange, L. Laporte, and W. E. Scott, The geomagnetic field, its description and analysis, pp. 3–4, *Carnegie Inst. Wash. Publ.* 580, 390 pp., Washington, D. C., 1947.